Exploration of optimal high-beta operation regime by magnetic axis swing in the Large Helical Device

S.Sakakibara 1), S.Ohdachi 1), K.Y.Watanabe 1), Y. Suzuki 1), H.Funaba 1), Y.Narushima 1), K.Ida 1), H.Chikaraishi 1), K.Toi 1), I.Yamada 1), K.Narihara 1), K.Tanaka 1), T.Tokuzawa 1), K.Kawahata 1), H.Yamada 1), A.Komori 1) and LHD Experiment Group 1)

1) National Institute for Fusion Science, Toki 509-5292, Japan

E-mail contact of main author: sakakibara.satoru@lhd.nifs.ac.jp

Abstract. In Large Helical Device (LHD), the volome averaged beta value $<\beta_{dia}>$ as high as 5.1 % was achieved in FY2007-2008 experiments. High beta operation regime was explored by the programmed control of magnetic axis position, which characterizes MHD equilibrium, stability and transport. This control became enable by increasing capability of poloidal coil power supply. The experiments made clear the effect of magnetic hill on MHD activities in high-beta plasmas with more than 4 %. Also it enabled to access the ideal stability boundary with keeping high-beta state. The strong m/n = 2/1 mode leading minor collapse in core plasma appeared with the inward shift of the magnetic axis.

1. Introduction

High beta plasma production is a common subject in magnetic confinement systems for a realization of an efficient fusion reactor, and an understanding of MHD characteristics concerning beta-limit is the most important issue. The magnetic axis position, R_{ax}, characterizing MHD stability as well as transport is one of key parameters for high-beta plasma production in stellarators/heliotrons. In the "standard" high-beta experiments of the Large Helical Device (LHD), high aspect ratio configuration has been selected for suppression of Shafranov shift because the outward shift decreases heating efficiency of neutral beam and increases helical ripple loss of particle. The achieved beta value has increased year by year, by increasing heating power of neutral beams in the optimized aspect-ratio configuration [1].

The previous high-β experiments in the "standard" configuration indicate that the clear limitation of the beta value due to disruptive phenomena has not been observed, whereas several notable phenomena caused by MHD instabilities have been observed when the beta value increased. In the medium $<\beta_{dia}>$ range of less than 3 %, the variation of plasma profiles with resonant magnetic fluctuations and the minor collapse caused by formation of steep pressure gradient in the vicinity of the resonant surface after pellet injection [2] have been observed in the core plasmas. It is found that these phenomena occur in marginal region against ideal interchange mode [3]. These MHD activities have not been observed when $<\beta_{dia}>$ is increased, which suggests that the resonant surface enters the magnetic well region due to finite-beta effects.

Investigating the impact of ideal stability boundary to the plasma is required for verifying the validity of linear MHD theory from a viewpoint of configuration optimization of fusion reactor. The LHD can produce the "ideally-unstable" configuration easily, for example, high plasma aspect ratio and/or the inward-shifted configurations. In the high aspect ratio configuration, the beta limit due to linear stability boundary could be decreased by enhanced magnetic hill and weak magnetic shear. In the experiments, strong m/n = 1/1 mode was excited in the low-beta regime and gave the large impact of plasma [4], where m and n are poloidal and toroidal numbers, respectively. In addition, plasma currents decreasing magnetic shear also excited the same mode and led the minor collapse in core. On the other hand, the extremely inward-shifted configuration destabilizes the mode in the low and/or medium beta range. The m/n = 2/1 mode excited in the core grew and led distortion of plasma profiles [5].

The real time movement of R_{ax} has been performed in FY2008, by increasing the capability of the power supply of poloidal coils for fast change of vertical magnetic flux. The purposes of this study are two things: further optimization of R_{ax} for high-beta plasma production and an access to the stability boundary with keeping high-beta state. This contributes to clarify the available operation regime and to extend accessible stability boundary. Here we report the results of R_{ax} swing experiments.

2. Experimental Setup

The magnetic configuration can be widely changed by using a pair of helical coil and three pairs of poloidal coils. The plasma aspect ratio, A_p, is set by changing the central position of helical coil current and R_{ax} is decided by the balance of poloidal coil currents. The inward shift of R_{ax} has an advantage of the transport property because of reduction of the amount of helical ripples, whereas it enhances magnetic hill destabilizing interchange modes. The previous experiments indicate that the highest energy confinement and beta value were obtained in the R_{ax} of 3.6 m configuration [1,6], and minor collapse due to core MHD instability occurred at R_{ax} = 3.5 m [5]. Therefore, we selected the R_{ax} range of 3.5-3.7 m in this experiments so as to investigate the configuration dependence of high-β characteristics.

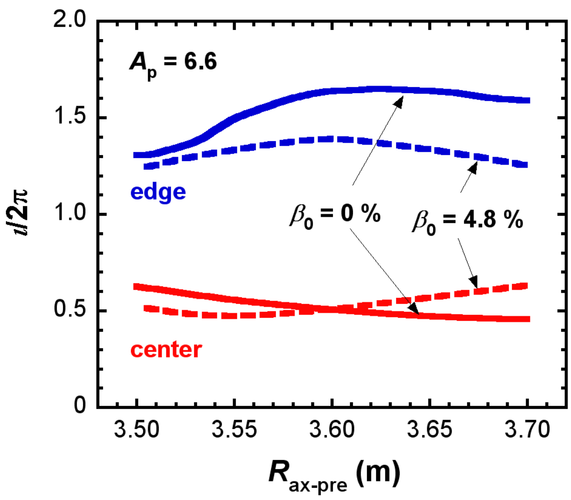

FIG. 1 Changes of plasma volume, edge and central rotational transforms as a function of vacuum R_{ax}.

The dependence of the positions of rational surfaces on $R_{ax\text{-}pre}$ is important for an excitation of MHD activity. Figure 1 shows the changes of edge and central rotational transforms, ι/2π, as a function of the preset magnetic axis position, $R_{ax\text{-}pre}$. In vacuum, edge ι/2π has a maximum at $R_{ax\text{-}pre}$ of 3.63 m and central ι/2π decreases from 0.65 to 0.45 with an increment of $R_{ax\text{-}pre}$. Note that the edge ι/2π is defined as that at the last closed flux surface (LCFS) and has higher values at the ergodic region outside LCFS because the ι/2π at the separatrix is 5. The finite-β equilibrium was calculated by VMEC [7] and the pressure profile was assumed as $P = P_0(1-\rho^2)(1-\rho^8)$, where ρ is defined as $(\Phi/\Phi_{edge})^{1/2}$, Φ and Φ_{edge} is the toroidal flux and that surrounded by the plasma edge, respectively. When the beta increases, the edge ι/2π decreases in any $R_{ax\text{-}pre}$ configuration, which means, for example, the

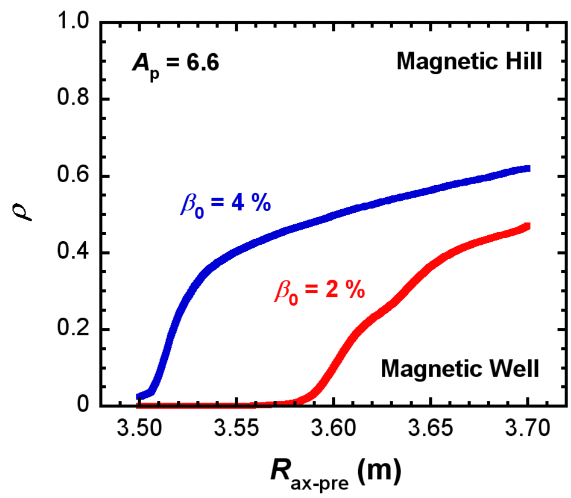

FIG.2 Magnetic well/hill boundaries in different beta value as a function of preset magnetic axis position.

$\iota/2\pi$ = 3/2 surface is pushed out to ergodic layer. The central $\iota/2\pi$ decreases at $R_{ax\text{-}pre}$ > 3.6 m and decreases at $R_{ax\text{-}pre}$ < 3.6 m. The key point is an existence of the $\iota/2\pi$ = 1/2 surface because the strong m/n = 2/1 mode appears when $R_{ax\text{-}pr}$ < 3.6 m.

The magnetic well/hill is one of essential parameters for stabilization of the MHD mode. The well/hill boundaries in the different beta cases are shown in Fig.2. The magnetic hill is formed in an entire region of plasma in vacuum. In the outward shifted plasma, magnetic well is easily formed from the plasma core compared to the inward shifted case. Especially, magnetic hill region is widely formed at $R_{ax\text{-}pre}$ of 3.5 m. In addition to this, weak magnetic shear in the core region destabilizes ideal interchange mode. The peripheral plasma has magnetic hill in any $R_{ax\text{-}pre}$ configuration even if the beta increases although strong magnetic shear is formed, which means that resistive interchange mode is a key instability in the periphery.

The capacity of power supply of poloical coils (PC) was increased in FY2008, which enables us to change R_{ax} during a discharge. The available voltage of PC power supply was extended from 33 V to 213 V. The $R_{ax\text{-}pre}$ can be changed from 3.6 m to 3.5 m for 1.4 s in the configuration with B_t of -0.425 T and A_p = 6.6 with keeping B_t.

3. Experimental Results

3-1. Typical R_{ax}-Swing Discharge

Figure 3 shows the comparison of discharges between with and without R_{ax} swing (reference) in the configuration with B_t = -0.425 T and A_p = 6.6. In both discharges, two co- neutral beams are applied at the beginning of discharge and a counter beam was added at 1.8 s. The total port-through power was 14.4 MW. The initial $R_{ax\text{-}pre}$ is 3.6 m in both cases, and $R_{ax\text{-}pre}$ was moved from 3.6 m at 1.02 s and approached 3.5 m at 3.02 s in the R_{ax} swing case. In the reference discharge, the R_{ax} estimated by T_e profile measurement with Thomson scattering system shifted to the outward and approached 3.85 m when the volume averaged beta value, $\langle\beta_{dia}\rangle$, was about 4.8 %, and the temporal movement of the R_{ax} depends on the $\langle\beta_{dia}\rangle$. The amount of the shift decreased with reduction of $R_{ax\text{-}pre}$ in the R_{ax} -swing case and R_{ax} was abruptly reduced at 2.24 s. This reduction is caused by drop of $\langle\beta_{dia}\rangle$, and no recovery of $\langle\beta_{dia}\rangle$ was observed to the end of discharge. While the central electron density, n_{e0}, gradually increased even before and after the collapse, central electron temperature, T_{e0}, abruptly dropped from 0.4 keV to 0.3 keV.

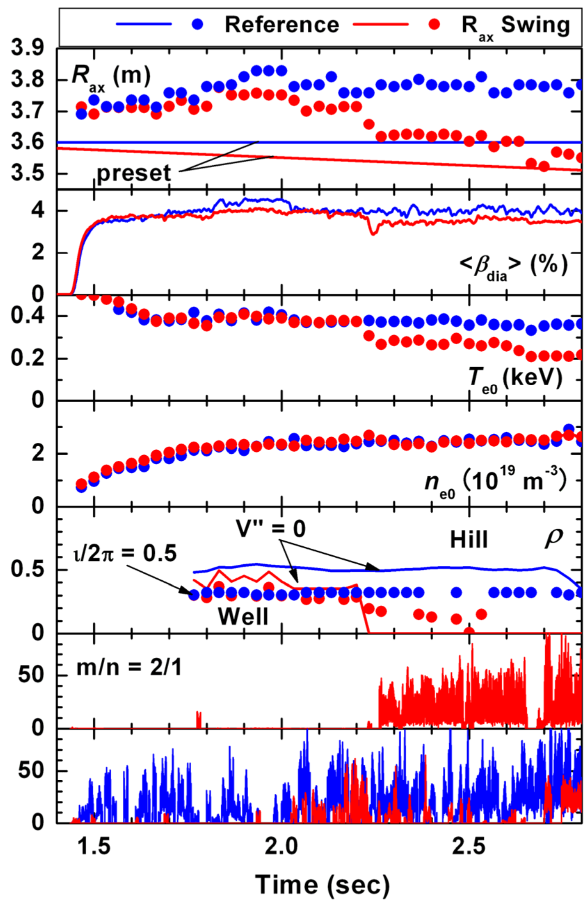

FIG. 3 Typical discharges with and without R_{ax} swing .

This degradation was caused in the core region and led by an excitation of $m/n = 2/1$ mode. In the reference, the magnetic well boundary ($V''=0$) was around $\rho = 0.5$, and the $\iota/2\pi = 0.5$ resonant surface is located in the magnetic well to the end of the discharge. In the R_{ax} swing case, although the resonance still remained inside the well boundary before 2.2 s, it went out of the well boundary with reduction of $R_{ax\text{-}pre}$ and magnetic well region was vanished after that. The $m/n = 2/1$ mode appeared at 2.24 s and the amplitude gradually increased. This tendency is consistent with reduction of magnetic Reynolds number due to temporal reduction (increment) of T_e (n_e) [1]. Figure 4 shows the T_e profiles at 2.0 and 2.3 s in the R_{ax} -swing discharge. The $\iota/2\pi = 0.5$ surface is predicted to be located at 3.35 m and 3.9 m. The flattening structure appeared around the resonance after the collapse, which led the reduction of $<\beta_{dia}>$ and the Shafranov shift.

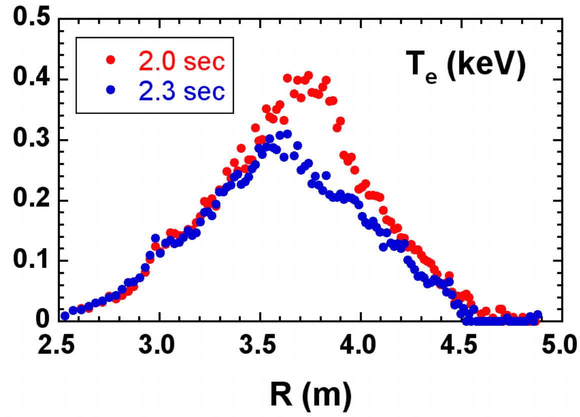

FIG.4 Electron temperature profiles at 2.0 and 2.3 s of R_{ax}-swing discharge.

The $m/n = 2/3$ mode excited in the periphery is one of the key instability in the high-beta and H-mode plasmas [8]. While the mode was observed with a large amplitude in the reference discharge, the mode was almost suppressed in the R_{ax}-swing discharge. However, there is no improvement of achieved beta (and/or plasma confinement) due to this suppression.

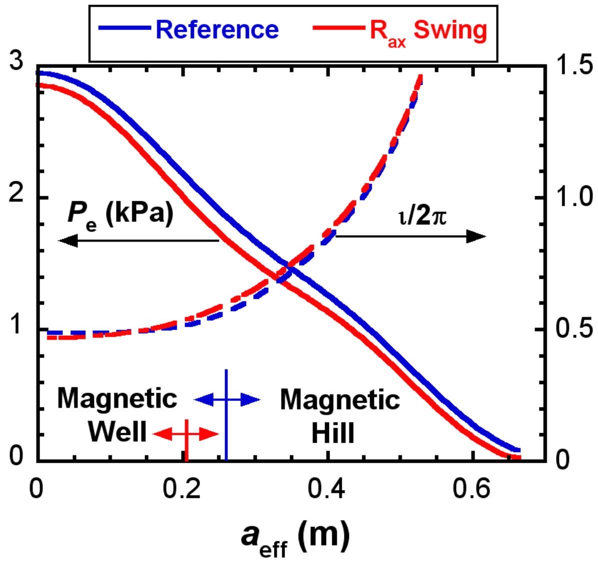

FIG.5 Electron pressure and rotational transform profiles at 2.2 s in the discharges with and without R_{ax}-swing.

Figure 5 shows the pressure and rotational transform profiles at 2.2 s, which corresponds to the time just before the collapse in the R_{ax} swing case. Both pressure profiles were almost the same in spite of different $R_{ax\text{-}pre}$, and the plasmas with $<\beta_{dia}>$ of about 4 % were realized in $R_{ax\text{-}pre} = 3.6$ m and 3.54 m as shown in Fig.3. Although the $\iota/2\pi$ profiles are almost similar in both cases, the magnetic well formation is different. Both $\iota/2\pi = 0.5$ surfaces are located in magnetic well region at this time. The $\iota/2\pi = 1.5$ resonance is located at $a_{eff} \sim 0.54$ m, where a_{eff} is an effective minor radius. The significant pressure gradient existed there in both cases, and the amplitude is almost the same at 2.2 s.

3-2. Appearance of low-*n* MHD Modes

The activities of $m/n = 2/1$ and 2/3 modes are summarized in Fig.6. The various operations with $R_{ax\text{-}pre}$ of 3.5 ~ 3.7 m are included in this figure. Note that the R_{ax} is the measurement value including Shafranov shift. The closed circle in the left figure corresponds to an appearance of the $m/n = 2/1$ mode and open circle is no observation. The mode appeared

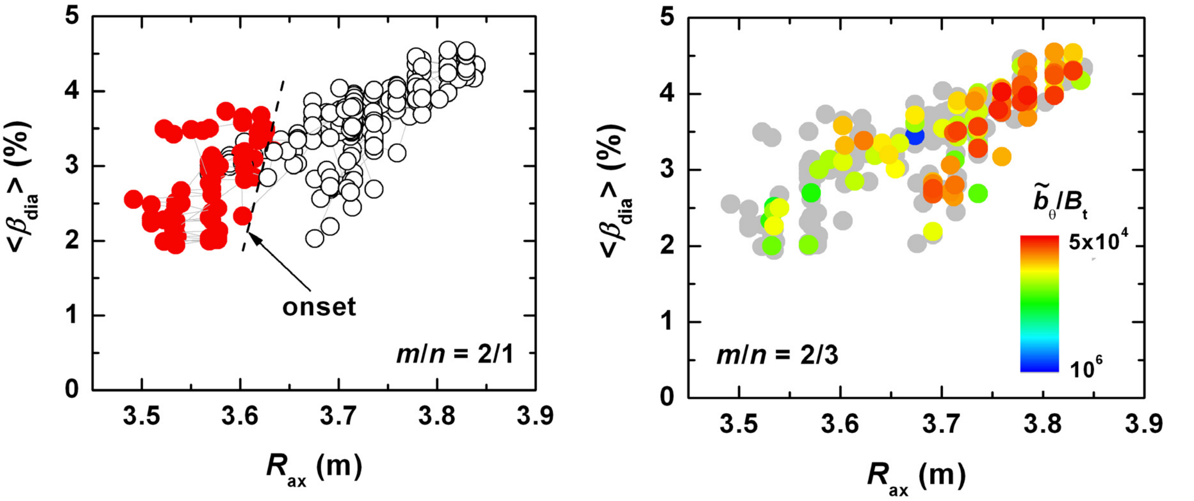

FIG.6 Appearance of m/n = 2/1 mode (left) and the amplitude of m/n = 2/3 mode (right) on the $<\beta_{dia}>$ and R_{ax} diagrams. The closed circle in the left figure means the appearance of the mode. The gray circle in the right figure is that the amplitude of the mode is less than 10^6.

in the R_{ax} range of 3.6 m around $<\beta_{dia}>$ of 2 %, and the onset extends to the outward of R_{ax} with the increment of $<\beta_{dia}>$. The right figure shows the dependence of the amplitude of the m/n = 2/3 mode on the $<\beta_{dia}>$ and R_{ax}. The mode appeared with large amplitude in the outward shift of the R_{ax}, and the amplitude of the mode decreased with the inward shift of R_{ax}.

3-3. Achieved Beta Value in Different R_{ax} Configurations

The changes of the $<\beta_{dia}>$ as a function of the preset of R_{ax} in several discharges are shown in Fig.7. The plasmas were produced under the conditions with the constant input power of neutral beams and toroidal field in order to find the optimal R_{ax} for high-beta plasma production. The circle means the plasma produced by gas-puff fueling. The closed and open circles correspond to discharges with and without R_{ax} swing, respectively. The achieved $<\beta_{dia}>$ gradually increased with R_{ax} and approached the maximum around 3.59 m. The $<\beta_{dia}>$ decreases when the R_{ax} exceeds 3.59 m. This tendency is predicted to be due to a reduction of heating efficiency and/or enhancement of particle and thermal transport (green dotted line). The solid star (★) indicates the maximum $<\beta_{dia}>$ obtained at the optimal R_{ax}. When the multiple pellet injections were applied to the R_{ax} = 3.59 m case, the $<\beta_{dia}>$ reached to as high as 5.1 % without the significant MHD activity (see Fig.8). The transport seems to play a role to limit the present beta value and it suggests that the higher beta value will be expected by the increase of heating power because of no degradation of achieved beta due to an increment of input power.

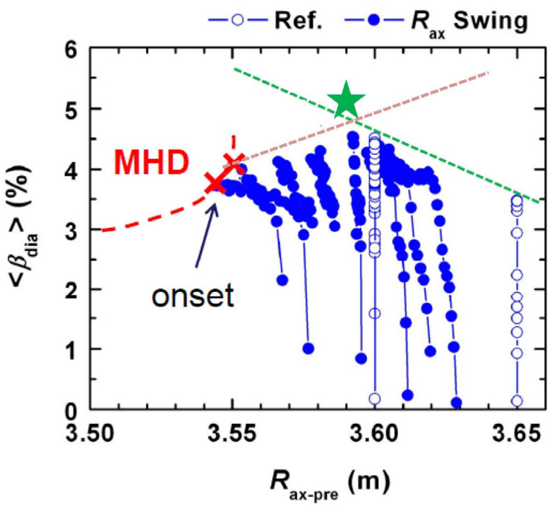

FIG.7 Achieved beta value in configurations with different R_{ax} configurations

The <β_{dia}> was decreased when the R_{ax} was shifted from 3.59 m to 3.55 m. The previous experiments suggest that peripheral MHD activities such as m/n = 2/3, 1/1 and so on are enhanced with the increment of <β_{dia}> and the reduction of magnetic Reynolds number [1]. Therefore, it had been anticipated that the inward shift of R_{ax} destabilized the mode further because of the increase in magnetic hill. However, as shown in fig.6, actual experiments showed that low-order MHD activities in the periphery were suppressed with the inward shift of R_{ax} even in the plasmas with the constant magnetic Reynolds number, and the peripheral MHD activities have a little effect on the reduction of <β_{dia}> with the inward shift of R_{ax}. Thus the main reason for reduction of <β_{dia}> with the inward shift of R_{ax}, is not due to low-order MHD activities, and R_{ax} dependences of the finite-β equilibrium, transport and so on have been investigated to clarify the reason (a beige dotted line).

In the R_{ax} range of less than 3.55 m, MHD activity excited in core region was enhanced and led to minor collapse, which limited the achieved beta value. As shown in fig.3 discharge, magnetic well region becomes narrow, and m/n = 2/1 mode is destabilized when the resonance moves to magnetic hill region with weak magnetic shear. When $R_{ax\text{-}pre}$ is set at 3.5 m, (that is, standard approach), m/n = 2/1 mode is easily destabilized at <β_{dia}> ~2 % [5], which corresponds to the case that "small" beta gradient drives the instability compared to the case of R_{ax} -swing.

3-4. Highest Beta Discharge

Finally, the discharge in configuration optimized to $R_{ax\text{-}pre}$, 3.59m, is shown in Fig.8. Four pellet were injected to the target plasma with <β_{dia}> of 1.5 %. The central electron pressure, P_{e0}, increased and decreased just after the injection, while <β_{dia}> kept the constant value of ~ 3.5 %. Just after the final injection, <β_{dia}> increased and reached 5.1 % and P_{e0} also approached the maximum at the same time. The R_{ax} was shifted to 3.88 m then. While the <β_{dia}> gradually decreased with time, P_{e0} increased and R_{ax} still remain the same position or was shifted to the outward. This is due to an increment of peaking factor of the pressure profile, which leads to Shafranov shift further. This tendency is a typical example of pellet discharge in LHD. In the medium beta discharge with 2 %, an enhancement of the profile peaking brings the plasma to ideal stability boundary and destabilizes core MHD instability [2].

The m/n = 1/1 mode is enhanced by the increment of the profile peaking. In this discharge, the amplitude of the mode gradually increased with time. On the other hand, m/n = 2/3 mode, which is dominant mode in the reference discharge with gas-

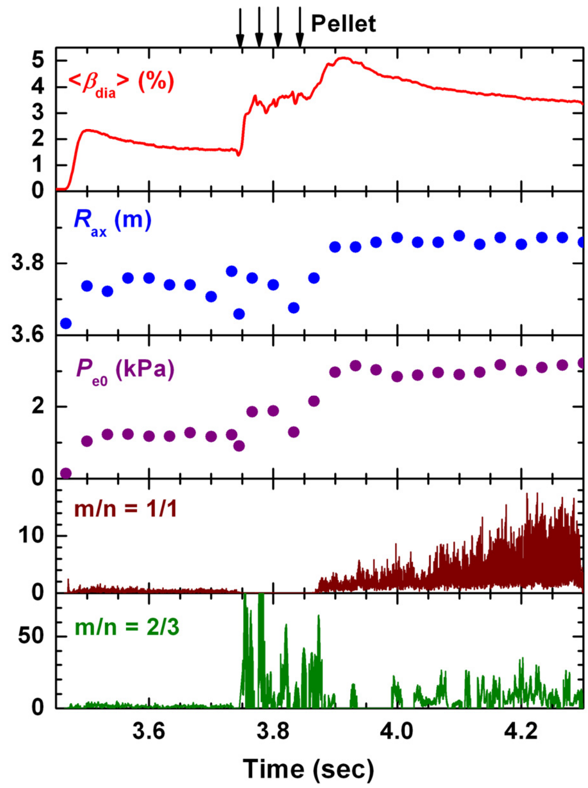

FIG.8 Highest beta discharge by multiple pellet injection in the optimized R_{ax} configuration.

puff fuelling shown in Fig.3, was enhanced during pellet injections. The mode vanished once and appeared again at 4 s. No m/n = 2/1 mode was observed in this discharge.

The profiles of pressure and rotational transform in gas-puff and pellet cases are compared in Fig.9. The profiles in the gas-puff case is the same as Fig.5 and the pellet case was obtained at 4.066 s in Fig.8 discharge. The $<\beta_{dia}>$ is about 4 % in both cases. In the pellet case, the steep pressure gradient was formed in the periphery with $\iota/2\pi$ = 1 and 1.5 resonances compared to the gas-puff case. The fact that the peaking factor increased with time is qualitatively consistent with the temporal behaviour of m/n = 1/1 mode.

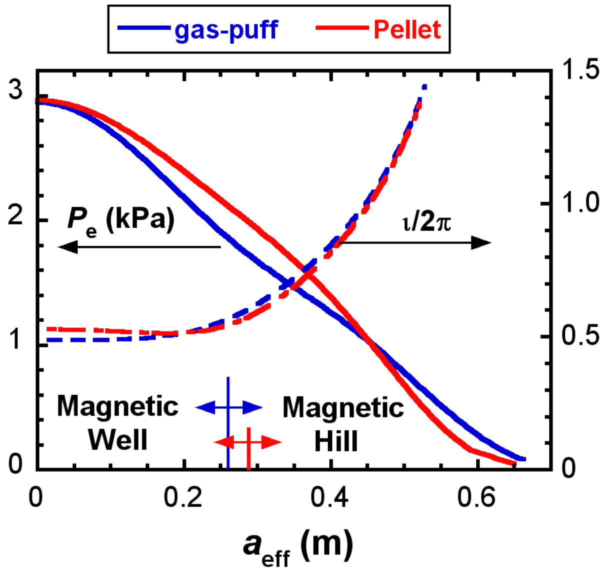

FIG.9 Electron pressure and rotational transform profiles in gas-puff and pellet cases.

4. Discussion and Summary

The optimal high-beta operation regime to the R_{ax} was found by real time R_{ax} swing, which contributes to achievement of $<\beta_{dia}>$ of 5.1 %. The experiments with the constant heating power suggest that the achieved $<\beta_{dia}>$ has different tendency at the inside and outside of the optimal R_{ax}, and the effect of MHD activities on it was investigated. Especially, the beta degradation inside the optimal R_{ax} cannot be interpreted by low-n MHD activities. Low-n MHD activities tend to be suppressed with the inward shift of R_{ax} except for core MHD, which means that low-n modes have a small effect on the achieved beta in ideal-stable regime. The previous high-beta experiments indicate that the energy confinement becomes worse with the increase in $<\beta_{dia}>$. This is due to the increment of the thermal transport in the periphery, which is predicted to be due to resistive-g mode turbulence [9,10]. Since this turbulence is enhanced by the magnetic hill as well as magnetic Reynolds number, one of the possibilities for the beta degradation is due to the enhancement of magnetic hill by the inward shift of R_{ax}.

The $<\beta_{dia}>$ limitation by core MHD activity was clearly observed in the inward shifted configuration, and the onset of the mode is qualitatively consistent with linear theory of ideal interchange mode. The R_{ax} swing technique enables us to find the new stability boundary on the beta and R_{ax} diagram by the access from high-beta state. In other words, core MHD activities are successfully observed in condition of different balance between driving term of ideal mode (pressure gradient) and magnetic configurations such as height of magnetic hill, strength of magnetic shear and so on. The mode led to the minor collapse in the core, whereas it was saturated with keeping profile flattening around the resonance. The effect on the plasma is localized and the mode causes no major disruption.

The edge instability with m/n = 2/3, which was dominantly observed in standard high-beta discharge and sometimes affects the plasma confinement, was suppressed with the inward shift of R_{ax}. This tendency can be interpreted by considering the movement of the resonance with R_{ax}. The resonance pushed out to the outward with the inward shift of R_{ax}, which leads to the decrease in the pressure gradient around resonance. According to numerical calculation of finite-beta equilibrium by using HINT2 code [11], edge magnetic field structure becomes to be disordered by finite-beta effect [1] and/or the inward shift of R_{ax}. The relationship between an excitation of edge instability, formation of pressure gradient and distortion of magnetic field structure is still open question, and the experimental verification have been proceeded from a viewpoint of so-called equilibrium beta limit in stellarator/heliotrons.

Acknowledgments

This work is supported by the NIFS under contract No NIFS05ULPP534 and the Ministry of Education, Science, Sports and Culture, Grant-in-Aid for Scientific Research (B), 19360419, 2009.

References

[1] SAKAKIBARA, S. et al., “MHD study of the reactor-relevant high-beta regime in the Large Helical Device”, *Plasma Phys. Control. Fusion* **50** (2008) 124014.
[2] SAKAKIBARA, S. et al., “Study of MHD Stability in LHD”, *Fusion Sci. Technol.* **58** (2010) 176-185.
[3] SAKAKIBARA, S. et al., “Effect of MHD activities on pressure profile in high-β plasmas of LHD”, *Plasma Phys. Control. Fusion* 44 (2002) A217.
[4] SAKAKIBARA, S. et al., “Recent Progress of MHD Study in High-Beta Plasmas of LHD” , *Fusion Sci. Technol.* **50** (2006) 177-185.
[5] SAKAKIBARA, S. et al., “Effects of Resonant Magnetic Fluctuations on Plasma Confinement in Current Carrying high-β Plasmas of LHD” , *Plasma Fusion Res.* **1** (2006) 003.
[6] YAMADA, H. et al., “Characterization of energy confinement in net-current free plasmas using the extended International Stellarator Database ” , *Nucl.Fusion* **45** (2005) 1684-1693.
[7] HIRSHMAN, S.P., RIJ, W.I.V. and MERKEL,P., “Three-dimensional free boundary calculations using a spectral Green’s function method ” , *Comput. Phys. Commun.***43** (1986) 143-155.
[8] TOI, K. et al., “Observation of the low to high confinement transition in the large helical device” , *Phys. Plasmas* **12** (2005) 020701.
[9] WATANABE, K.Y. et al., “Effects of global MHD instability on operational high-beta regime in LHD” , *Phys. Plasmas* **45** (2005) 1247-1254.
[10] FUNABA, H. et al., “Local Transport Property of Reactor-Relevant High-Beta Plasmas on LHD” , *this conference*
[11] SUZUKI, Y. et al., “Development and application of HINT2 to helical system plasmas” , *Nucl. Fusion* **46** (2006) L19-L24.